The chemical chaperone 4-phenylbutyric acid prevents alcohol-induced liver injury in obese KK-A^y mice

Maiko Suzuki[1], Kazuyoshi Kon[1], Kenichi Ikejima[1], Kumiko Arai[1], Akira Uchiyama[1], Tomonori Aoyama[1], Shunhei Yamashina[1], Takashi Ueno[2], and Sumio Watanabe[1]

[1]Department of Gastroenterology, Juntendo University Graduate School of Medicine, 2-1-1 Hongo, Bunkyo-ku, Tokyo, 113-8421 Japan

[2]Laboratory of Proteomics and Medical Science, Research Support Center, Juntendo University Faculty of Medicine, 2-1-1 Hongo, Bunkyo-ku, Tokyo, 113-8421 Japan

Short title: PBA prevents alcoholic liver injury

Corresponding author: Kazuyoshi Kon, MD, PhD, FAASLD. 2-1-1 Hongo, Bunkyo-ku, Tokyo, 113-8421 Japan. Phone: +81-3-3813-3111, fax: +81-3-3813-8862, e-mail: kazukon@juntendo.ac.jp

Financial support

This work was supported in part by the Japan Society for the Promotion of Science

19 KAKENHI (no. 15K09023 to K.I. and no. 16H05293 to S.W.) and a Grant for Cross-
20 disciplinary Collaboration, Juntendo University (no. 28-39).

Abstract

Background: Co-occurrence of metabolic syndrome and chronic alcohol consumption is increasing worldwide. The present study investigated the effect of the chemical chaperone 4-phenylbutyric acid (PBA)—which has been shown to alleviate dietary steatohepatitis caused by endoplasmic reticulum (ER) stress—on chronic-plus-binge ethanol (EtOH)-induced liver injury in a mouse model of obesity.

Methods: Male KK-A^y mice (8 weeks old) were fed a Lieber–DeCarli diet (5% EtOH) for 10 days. Some mice were given PBA intraperitoneally (120 mg/kg body weight, daily) during the experimental period. On day 11, mice were gavaged with a single dose of EtOH (4 g/kg body weight). Control mice were given a dextrin gavage after being pair-fed a control diet. All mice were then serially euthanized before or at 9 h after gavage.

Results: Chronic-plus-binge EtOH intake induced massive hepatic steatosis along with hepatocyte apoptosis and inflammation, which was reversed by PBA treatment. Administration of PBA also suppressed chronic-plus-binge EtOH-induced upregulation of ER stress-related genes including *binding immunoglobulin protein* (*Bip*), unspliced and spliced forms of *X-box-binding protein-1* (*uXBP1* and *sXBP1*, respectively), *inositol trisphosphate receptor* (*IP3R*), and *C/EBP homologous protein* (*CHOP*). Further, it blocked chronic-plus-binge EtOH-induced expression of the oxidative stress marker

heme oxygenase-1 (*HO-1*) and 4-hydroxynonenal. Chronic EtOH alone (without binge) increased *Bip* and *uXBP1*, but it did not affect those of *sXBP1*, *IP3R*, *CHOP*, or *HO-1*. PBA reversed the pre-binge expression of these genes to control levels, but it did not affect chronic EtOH-induced hepatic activity of cytochrome P450 2E1.

Conclusion: Binge EtOH intake after chronic consumption induces massive ER stress-related oxidative stress and liver injury in a mouse model of obesity through dysregulation of the unfolded protein response. PBA ameliorated chronic-plus-binge EtOH-induced liver injury by reducing ER and oxidative stress after an EtOH binge.

Keywords: alcoholic liver disease, obesity, metabolic syndrome, ER stress, oxidative stress

50 **Introduction**

51 Chronic alcohol consumption is a common cause of chronic liver disease worldwide,
52 leading to alcoholic liver steatosis, cirrhosis, and hepatocellular carcinoma (Rehm et al.,
53 2013). The pathophysiology of alcoholic liver disease can include acute-on-chronic liver
54 injury, which in severe cases has a short-term mortality of 25%–45% at 1 month
55 (Akriviadis et al., 2000; Imperiale and McCullough, 1990; Mathurin et al., 2011; Yu et
56 al., 2010). The recent obesity pandemic in developed countries has increased the risk of
57 non-alcoholic fatty liver disease, which overlaps with the risk of liver disease posed by
58 alcohol consumption (Mahli and Hellerbrand, 2016; Watanabe et al., 2015a, b). Metabolic
59 syndrome increases the risk of liver injury as well as morbidity and mortality related to
60 liver injury due to chronic alcohol consumption (Almeda-Valdes et al., 2016; Hellerbrand,
61 2010; Naveau et al., 1997; Raff et al., 2015; Tsukamoto, 2007). Although absolute
62 abstinence from alcohol is the best way to prevent alcoholic liver diseases (Bergheim et
63 al., 2005), it is often impossible.

64 Several studies have shown that endoplasmic reticulum (ER) stress contributes to
65 the development of alcoholic liver disease (Dara et al., 2011; Fernandez et al., 2013; Ji,
66 2015; Ji and Kaplowitz, 2003; Malhi and Kaufman, 2011; Tan et al., 2013). ER stress and
67 activation of the unfolded protein response (UPR) is caused by accumulation of unfolded

proteins in the ER, a cellular organelle that is important for the regulation of calcium homeostasis, lipid metabolism, and protein synthesis. The UPR pathway includes induction of several molecular chaperones that restore cellular homeostasis by promoting the folding or degradation of unfolded proteins; however, if ER stress is prolonged or too severe, the signaling switches from pro-survival to pro-death, leading to ER stress-induced apoptosis (Malhi and Kaufman, 2011). The chemical chaperone 4-phenylbutyric acid (4-PBA) is a drug approved by the U.S. Food and Drug Administration that alleviates ER stress by assisting in protein folding (Roy et al., 2015). We previously reported that PBA prevents murine dietary steatohepatitis caused by *trans*-fatty acids plus fructose by minimizing ER stress (Morinaga et al., 2 015). However, it is not known whether PBA can prevent EtOH-induced liver injury overlapping with metabolic steatohepatitis via a similar mechanism.

Most murine models of alcoholic liver injury include free access to the Lieber–DeCarli liquid ethanol (EtOH)-containing diet (Gustot et al., 2006; Hritz et al., 2008; Kang et al., 2009; Petrasek et al., 2012; Roychowdhury et al., 2009; Shen et al., 2010), but this induces only liver micro-steatosis and a slight elevation of serum alanine transaminase (ALT) level. Short-term chronic EtOH feeding combined with a single EtOH binge (chronic-plus-binge EtOH or National Institute on Alcohol Abuse and

Alcoholism model) was recently proposed as an alternative. This model results in significant ALT elevation, fat accumulation, and neutrophil infiltration into the liver, which mimics acute-on-chronic alcoholic liver injury in humans; however, changes in hepatic histology are limited in some animals (Bertola et al., 2013). KK-A^y mice are a congenic strain in which the A^y allele at the *agouti* locus had been transferred to the inbred KK strain by repeated backcrossing. KK-A^y mice are a suitable model of steatohepatitis with metabolic syndrome because they spontaneously develop obesity along with hyperglycemia, hyperinsulinemia, and steatohepatitis (Kon et al., 2017; Takashima et al., 2016; Yamagata et al., 2013). We previously reported that KK-A^y mice exhibit increased susceptibility to acetaminophen-induced liver injury or dietary steatohepatitis and fibrosis (Kon et al., 2010). In the present study, we investigated the effect of PBA on chronic-plus-binge-alcoholic liver injury using obese KK-A^y mice.

Methods

Materials

The Liber–DeCarli liquid diet was purchased from Dyets, Inc. (Bethlehem, PA, USA). PBA was purchased from Sigma-Aldrich (St. Louis, MO, USA). Anti-4-hydroxy-2-nonenal (4-HNE) primary antibody was purchased from Abcam (Cambridge, MA,

USA). Biotinylated anti-mouse IgG secondary antibody was purchased from Santa Cruz Biotechnology (Dallas, TX, USA). Anti-M30 CytoDeath antibody, streptavidin-β-peroxidase, and protease inhibitor cocktail (Complete Mini) were purchased from Roche Diagnostics (Basel, Switzerland). Secondary HRP-anti-mouse IgG, anti-C/EBP homologous protein (CHOP) antibody, and anti-glyceraldehyde 3-phosphate dehydrogenase (GAPDH) antibody were purchased from Cell Signaling Technology Inc. (Danvers, MA, USA). Isoflurane was purchased from Pfizer (New York, NY, USA). All other reagents were from Sigma-Aldrich, unless otherwise specified.

Animals and experimental design

All experimental protocols were approved by the Committee of Laboratory Animals following institutional guidelines. KK-A^y mice were purchased from CLEA Japan (Tokyo, Japan) and housed in air-conditioned, specific pathogen-free animal quarters, with lighting from 08:00 to 20:00 h. The mice were given unrestricted access to standard laboratory chow and water until the start of the study.

Starting at 8 weeks of age and after acclimation, male KK-A^y mice were fed Lieber–DeCarli liquid diet containing 5% EtOH, or they were pair-fed a control diet containing isocaloric maltodextrin for 10 days. Some mice were given intraperitoneal

injections of PBA (120 mg/kg body weight, daily) during the feeding period. Saline, as the PBA vehicle, was intraperitonealy administered to control mice during the same period. On day 11, some mice received a single gavage of EtOH (4 g/kg body weight) or isocaloric maltodextrin as a control. Animals were anesthetized by inhalation of isoflurane mixed with oxygen and air and euthanized by exsanguination 0–9 h later. Liver tissue and serum samples were collected at this time from each group (n = 5). To compare the effects of chronic-plus-binge EtOH on liver histology, chronic-plus-binge EtOH treatment was also performed on nonobese and nondiabetic C57Bl/6J mice, which are the offspring of two generations preceding that of the KK-A^y mice, were treated with chronic-plus-binge EtOH. Nine hours following a single gavage of EtOH (5 g/kg body weight), the mice were sacrificed.

Triacylglycerol assay

Triacylglycerol concentration in liver tissue was determined using an Adipogenesis Colorimetric/Fluorometric Assay Kit (BioVision, San Francisco, CA), and the absorbance at 570 nm was measured using the Molecular Devices SpectraMax® 340 (Molecular Devices, Sunnyvale, CA).

Serum AST, ALT, triglyceride, and glucose levels

Serum AST/ALT activity and triglyceride levels were measured colorimetrically using the Fuji DRI-CHEM system (Fujifilm, Tokyo, Japan). Blood glucose levels were measured using a blood glucose meter (Glutest, Sanwa Kagaku Kenkyusho, Nagoya, Japan).

Histological analysis and immunohistochemistry

For histological evaluation, liver tissue specimens were fixed in 10% buffered formalin, embedded in paraffin, sectioned, and stained with hematoxylin and eosin (H-E). The expression and localization of 4-HNE in liver tissue was evaluated by immunohistochemistry as previously described (Okumura et al., 2006). Briefly, deparaffinized tissue sections were incubated with monoclonal anti-4-HNE antibody followed by secondary biotinylated anti-mouse IgG. Subsequently, binding was visualized using an avidin–biotin complex solution followed by incubation with a 3,3-diaminobenzidine tetrahydrochloride solution (Vectastain Elite ABC kit; Vector Laboratories, Burlingame, CA, USA).

The M30 CytoDeath assay, which labels the caspase cleavage product cytokeratin 18 (ccCK18), was performed according to the manufacturer's instructions. Briefly,

deparaffinized tissue sections were incubated with a monoclonal anti-M30 antibody and secondary biotinylated anti-mouse IgG, and specific binding was visualized as described above. All histological and immunohistochemical specimens were observed with an optical microscope (DM7000; Leica, Wetzlar, Germany) equipped with a digital camera (MC120HD; Leica). Counts were randomly obtained from each slide, with at least 1000 hepatocytes counted in all cases. 4HNE-positive and ccCK18-positive cells were identified, and positive cells were expressed as a percentage of the total number of cells counted.

RNA preparation and real-time reverse transcription quantitative PCR (qPCR)

Total RNA was isolated from frozen tissue samples using an Illustra RNAspin Mini RNA Isolation kit (GE Healthcare, Waukesha, WI, USA). The concentration and purity of the isolated RNA were assessed by measuring the optical density at 260 and 280 nm. For qPCR, total RNA (1 μg) was reverse transcribed using Moloney murine leukemia virus transcriptase (SuperScript II; Invitrogen, Carlsbad, CA, USA) and an oligo(dT)12–18 primer at 42°C for 1 h. The cDNA (1 μg) was used as a template for target gene amplification using Fast SYBR Green Master Mix (Applied Biosystems, Foster City, CA, USA) and specific primers for each gene (Table 1).

The reaction was performed with a 10-s activation at 95°C, followed by 40 cycles of 95°C for 5 s and 60°C for 31 s, and a final cycle of 95°C for 15 s, 60°C for 1 min, and 95°C for 15 s on an ABI PRISM 7700 sequence detection system (Applied Biosystems). Obtained threshold cycle values were used to calculate the relative expression level of target genes.

Preparation of total proteins

Total protein extracts were obtained by homogenizing frozen tissues in a buffer containing 50 mM Tris (pH 8.0), 150 mM NaCl, 1 mM ethylenediaminetetraacetic acid (EDTA), 1% Triton X-100, and protease inhibitors (Complete Mini®), followed by centrifugation at 17,400×g for 15 min. The protein concentration was determined using a Bio-Rad protein assay kit (Bio-Rad Laboratories, Hercules, CA, USA).

Western blotting

Protein extracts (50 μg) were electrophoresed in 12% sodium dodecyl sulfate (SDS) polyacrylamide gels and electrophoretically transferred onto polyvinylidene fluoride membranes. The membranes were then blocked with 5% nonfat dry milk in Tris-buffered saline, and incubated with primary antibodies against CHOP (anti-rabbit, 1:500)

or GAPDH (anti-rabbit, 1:1000), followed by a secondary horseradish peroxidase-conjugated anti-rabbit IgG. Specific bands were then visualized using the ECL prime detection kit (GE Healthcare, Waukesha, WI, USA) and detected using an LAS3000 imaging system (Fuji Film, Japan).

CYP2E1 activity assay

Cytochrome P450 2E1 (CYP2E1) activity was determined with liver homogenates using p-nitrophenol as a substrate, according to a previously described procedure (Cederbaum AI, 2014). In brief, mouse liver specimens (each ~0.15 g) were suspended with 1 mL of extraction buffer containing 5 mM TES-NaOH (pH 7.4), 0.3 M sucrose, and proteinase inhibitor cocktail (Nacalai Tesque, Kyoto, Japan), and homogenized with a glass/Teflon homogenizer (5-8 up-down strokes). The homogenate was incubated with a mixture containing 0.1 M KH_2PO_4-NaOH (pH 7.2), 0.2 mM p-nitrophenol, and 1 mM NADPH for 15 min. The reaction was terminated by adding 30% TCA to achieve a final concentration of 1.5% TCA. The suspension was centrifuged at 2,000 ×g for 15 min. Finally, the resultant supernatant (0.85 mL) was mixed with 0.15 mL of 10M NaOH, and the absorbance was immediately read at 510 nm, corresponding to the wavelength of the reaction product (p-nitrocatechol).

Statistical analysis

Data are expressed as mean ± SEM. Differences between mean values were evaluated by one-way analysis of variance (ANOVA) or Kruskal–Wallis ANOVA on ranks followed by the Student–Newman–Keuls pairwise multiple comparisons test as appropriate. A significance level of $P < 0.05$ was selected prior to analysis.

Results

PBA suppresses the hepatic steatosis, inflammation, and early apoptosis caused by chronic-plus-binge EtOH intake

During the study period, there was no significant body weight change in the mice of any group, and the obesity phenotype was maintained with a weight around 36 g at the time of sacrifice (Fig. 1A). Hyperglycemia (>300 mg/dL) was observed in mice of the control group although the blood sugar level showed a decreased tendency in the group treated with EtOH. However, there was no statistically significant difference in blood sugar levels among the groups, and all mice still showed hyperglycemia (>250 mg/dL). Treatment with PBA did not affect blood sugar levels (Fig. 1B). In contrast, EtOH administration induced marked hypertriglyceridemia in line with previous reported, and the serum

230 triglyceride levels were significantly decreased by PBA ($P < 0.05$, Fig 1C). H-E staining
231 of liver tissue sections revealed that chronic-plus-binge EtOH feeding induced severe
232 hepatic steatosis accompanied by neutrophil infiltration around the central veins 9 h after
233 the EtOH binge, in contrast to the minimal hepatic steatosis observed in the chronic-plus-
234 binge EtOH C57Bl/6 mouse model (Fig. 1D and G, Supplementary Fig. 1). Treatment
235 with PBA alleviated these pathological effects (Fig. 1F). PBA significantly reduced the
236 EtOH-induced hepatic triglyceride content (Fig 1H). Moreover, the mean serum AST
237 and ALT levels at 9 h after the EtOH binge were significantly elevated as compared to
238 those in isocaloric dextrin-gavaged control mice, respectively ($P < 0.05$), and treatment
239 with PBA significantly ($P < 0.05$) suppressed this increase in serum AST and ALT levels
240 (Fig. 1I and J). Hepatocytes undergoing apoptosis were also observed by
241 immunohistochemical detection of ccCK18. There were significantly more ccCK18-
242 positive cells in the EtOH binge group than in controls ($P < 0.05$), and treatment with
243 PBA decreased the percentage of ccCK18-positive cells close to control levels ($P < 0.05$,
244 Fig. 2A–D). PBA also blocked the mRNA expression of tumor necrosis factor α (*TNFα*)
245 and interleukin 6 (*IL6*), which were upregulated in the livers of chronic-plus-binge EtOH-
246 fed mice (Fig. 2E, F).
247

PBA prevents chronic-plus-binge EtOH feeding-induced ER stress

The expression of ER stress markers was evaluated by qPCR. Binding immunoglobulin protein (*BiP*) expression was increased 3-fold in the liver of chronic-plus-binge EtOH-fed mice relative to controls. Treatment with PBA reversed this effect ($P < 0.05$) (Fig. 3A). Similarly, hepatic expression of *unspliced XBP1* (*uXBP1*) and *spliced XBP1* (*sXBP1*) transcripts was increased by chronic-plus-binge EtOH feeding to 2.6 ± 0.8 and 2.2 ± 0.1, respectively, relative to control mice ($P < 0.05$), but the levels were reduced to 1.5 ± 0.2 and 1.1 ± 0.1, respectively, by PBA administration (Fig. 3B, C). The expression of *inositol 1,4,5-trisphosphate receptor type 1* (*IP3R1*) in the liver was increased by chronic-plus-binge EtOH intake as compared to control mice (1.8 ± 0.2; $P < 0.05$), but it was downregulated by PBA treatment (1.4 ± 0.1; $P < 0.05$). Finally, the increase in the mRNA level of *CHOP*—a key signal for ER stress-related apoptosis—in the livers of chronic-plus-binge EtOH-fed as compared to control mice (5.1 ± 0.6, $P < 0.05$) was reversed by PBA treatment (2.9 ± 0.6; $P < 0.05$) (Fig. 3D, E). CHOP protein expression was also evaluated. EtOH dramatically increased CHOP protein levels, over 40 times of controls, and PBA significantly decreased the EtOH-induced CHOP expression (Fig. 3F).

PBA suppresses oxidative stress induced by chronic-plus-binge EtOH intake

Oxidative stress in hepatocytes after chronic-plus-binge EtOH feeding was evaluated by immunohistochemical detection of 4-HNE. Chronic-plus-binge EtOH consumption increased the proportion of 4-HNE-positive cells relative to control mice (21.4 ± 3.5% vs. 0.2 ± 0.0%; $P < 0.05$). In PBA-treated mice, the increase in the 4-HNE-positive fraction was smaller (12.1 ± 2.5%; $P < 0.05$) (Fig. 4A–D). Hepatic mRNA expression of *heme oxygenase-1* (*HO-1*), another oxidative stress marker, was increased to 14.0 ± 0.9 relative to controls by chronic-plus-binge EtOH intake ($P < 0.05$), an effect that was abrogated by PBA (8.1 ± 1.9; $P < 0.05$) (Fig. 4E).

Chronic EtOH consumption causes ER stress but does not induce oxidative stress or increase serum ALT levels

We evaluated the mechanisms underlying alcoholic liver injury caused by chronic alcohol consumption before binge EtOH consumption. *BiP* and *uXBP1* mRNA expression was increased in the mouse liver after chronic EtOH feeding even without EtOH binging to 2.0 ± 0.3 and 2.0 ± 0.4, respectively ($P < 0.05$). However, treatment with PBA suppressed the levels to 1.1 ± 0.1 and 1.1 ± 0.1, respectively ($P < 0.05$). In contrast, *sXBP1*, *IP3R1*, and *CHOP* transcript expressions were unchanged by chronic EtOH feeding, which also had no effect on serum AST/ALT or hepatic *HO-1* mRNA levels (Fig. 5A-E and G-I).

284 CHOP protein levels also showed no significant increase in the EtOH group (Fig. 5F).
285 The expression of *CYP2E1* mRNA was upregulated to 2.6 ± 0.1 relative to control mice
286 by chronic EtOH intake ($P < 0.05$), which was not improved by PBA treatment (Fig. 6A).
287 PBA did not affect the activity of CYP2E1 enhanced by chronic-EtOH administration
288 (Fig. 6B).
289

290 **Discussion**

291 In this study, we developed an animal model of alcoholic liver injury by chronic-plus-
292 binge EtOH feeding to obese KK-A^y mice. The mice developed severe hepatic steatosis
293 around the central veins, accompanied by increased hepatocyte apoptosis and serum AST
294 and ALT levels as compared to those of their pair-fed controls mice. (Fig. 1D-F). Since
295 the KK-A^y mice used in this study were relatively young, the fatty liver inflammation was
296 minor, despite the presence of hyperglycemia and obesity in the control group. These
297 mice maintained the phenotype of obesity and hyperglycemia even under EtOH exposure;
298 thus, the established animal model is considered to be useful as a model of alcoholic liver
299 injury with a background of obesity and hyperglycemia. Although PBA treatment did not
300 affect the hyperglycemia, it reduced serum triglyceride levels and the triglyceride content
301 in the liver tissue. ER stress was reported to cause impairment of lipid metabolism (Zhou

et al. 2014); thus, the suppression of ER stress by PBA likely contributed to the improvement of lipid metabolism. Immunohistochemical detection of ccCK18 and qPCR analysis of *Tnfα* and *Il6* transcript levels revealed the induction of hepatocyte apoptosis and hepatic inflammation, respectively. Thus, the mouse model developed in this study appropriately recapitulates the features of alcohol-induced steatohepatitis. Notably, treatment with PBA dramatically improved these pathophysiological changes.

ER and oxidative stress are associated with various types of liver injuries (Hamano et al., 2014; Kusama et al., 2017; Sasaki et al., 2015), including alcoholic liver disease (Dara et al., 2011; Malhi and Kaufman, 2011; Szuster-Ciesielska et al., 2013; Yamashina et al., 2005). In this study, chronic-plus-binge EtOH consumption increased the hepatic mRNA expression levels of ER stress markers such as *Bip*, *uXbp1*, *sXbp1*, *Ip3r*, and *Chop,* as well as CHOP protein levels. BiP is an ER-resident chaperone that inhibits UPR activation by binding to both unfolded proteins and ER stress sensor luminal domains (Bertola et al., 2013; Gulow et al., 2002). Under conditions of ER stress, *XBP1* mRNA is efficiently spliced to a functional form, and sXBP1 activates its target genes, including those encoding factors that function in ER protein folding and quality control. Thus, sXBP1 is considered to play a protective role against ER stress-related injury, although XBP1 action can vary according to the cell type. CHOP is an important

contributor to ER stress-mediated apoptosis (Yamaguchi and Wang, 2004). IP3R is a calcium-release channel on the ER membrane that relays calcium signals locally from the ER to mitochondria, which is essential for induction of the mitochondrial apoptosis pathway (Kiviluoto et al., 2013). Immunohistochemical detection of 4-HNE and qPCR analysis of *Ho1* mRNA expression revealed that PBA reversed the oxidative stress induced by chronic-plus-binge EtOH feeding in the livers of KK-A^y mice. These findings indicate that chronic-plus-binge EtOH consumption increases ER stress, which induces both protective and pathogenic signals to ultimately promote the apoptosis of hepatocytes through CHOP activation. This in turn leads to calcium release from IP3R on the ER to mitochondria to increase oxidative stress. Thus, treatment with PBA prevented liver injury by inhibiting this cascade of events via suppression of ER stress.

Chronic EtOH consumption without binging did not increase serum ALT levels as previously reported (Bertola et al., 2013). We also did not observe an elevation of *sXbp1*, *Chop*, or *Ho-1* transcripts in our model. However, chronic EtOH induced *Bip* and *uXbp1* overexpression, which was reversed by PBA treatment. It has been reported that an EtOH binge alone does not induce liver injury (Bertola et al., 2013); thus, in the chronic-plus-binge EtOH model, the chronic phase of EtOH intake is essential for induction of liver injury, even if it does not cause any liver injuries itself. Our data indicate that chronic

338 EtOH consumption (before EtOH binge) results in the non-lethal accumulation of
339 unfolded proteins that induce BiP and uXBP1 but not downstream UPR proteins such as
340 sXBP1, IP3R, or CHOP. The cell death associated with ER stress is not a simple one-way
341 process. Although CHOP is the most powerful factor to induce ER stress-related cell
342 death, cell death does not occur by activation of CHOP alone, suggesting the involvement
343 of other complementary signals (Han et al. 2013; Hiramatsu et al. 2014; Gurlo et al. 2016;
344 Southwood et al. 2016). Our findings suggest that sustained mild ER stress during chronic
345 EtOH plays a key role as the first step in this crucial process after an EtOH binge. PBA
346 prevented liver injury after chronic-plus-binge EtOH intake, possibly by reducing the ER
347 stress during the chronic EtOH phase, followed by blocking lethal ER stress signals such
348 as IP3R and CHOP activation.

349 The relationship between oxidative and ER stress is controversial (Adachi et al.,
350 2014; Kon et al., 2010; Malhi and Kaufman, 2011; Rolo et al., 2012; Tilg and Moschen,
351 2010): the former can induce the latter and vice versa (Back et al., 2009; Malhotra et al.,
352 2008). Based on the results of this study, we propose that severe EtOH-induced liver
353 injury is associated with hypersensitivity to oxidative stress caused by increased ER
354 stress: in this scenario, the latter occurs upstream of the former. We previously reported
355 that *trans*-fatty acids induce ER stress and increase the susceptibility to oxidative stress

356 in mouse hepatocytes (Morinaga et al., 2015). Thus, chronic EtOH consumption may
357 cause liver injury via similar mechanisms.

358 The enzymes alcohol dehydrogenase, CYP2E1, and catalase all contribute to the
359 oxidative metabolism of EtOH (Cederbaum, 2012). In this study, we examined the effect
360 of PBA on *Cyp2e1* expression, because overexpression of CYP2E1 induced by chronic
361 EtOH consumption has been considered to enhance EtOH-induced oxidative stress and
362 liver injury (Abdelmegeed et al., 2013; Wu et al., 2012; Yang et al., 2012). CYP2E1 is
363 primarily localized in the ER but is also expressed in mitochondria (Leung and Nieto,
364 2013). In this study, chronic EtOH consumption increased both the hepatic mRNA
365 expression level of *Cyp2e1* and CYP2E1 activity, and these effects were not reversed by
366 PBA. These findings suggest that the protective effect of PBA on chronic-plus-binge
367 EtOH-induced steatohepatitis is, at least in part, independent of activation of CYP2E1-
368 related EtOH metabolism during chronic EtOH consumption.

369 In conclusion, the results of this study demonstrate that chronic-plus-binge EtOH
370 intake resulted in the development of steatohepatitis and enhanced ER and oxidative
371 stress in KK-A^y mice. PBA treatment improved hepatic apoptosis and inflammation by
372 reducing sustained ER stress during the chronic phase, and the rapid increase of ER stress
373 and oxidative stress after EtOH binging. Our findings suggest that the ER stress pathway

374 plays a key role in the development of alcoholic liver injury. Further, the components of
375 this pathway are potential therapeutic targets for the management and prevention of
376 alcoholic liver disease.
377

378 **Acknowledgments**
379 The authors thank Takako Ikegami and Tomomi Ikeda (Laboratory of Molecular and
380 Biochemical Research, Research Support Center, Juntendo University Graduate School
381 of Medicine, Tokyo, Japan) for technical assistance.
382

383 **Conflict of interest**
384 The authors have no conflicts of interest to declare.

385 **References**

386 Abdelmegeed MA, Banerjee A, Jang S, Yoo SH, Yun JW, Gonzalez FJ, Keshavarzian A,
387 Song BJ (2013) CYP2E1 potentiates binge alcohol-induced gut leakiness,
388 steatohepatitis, and apoptosis. Free Radic Biol Med 65:1238–1245.

389 Adachi T, Kaminaga T, Yasuda H, Kamiya T, Hara H (2014) The involvement of
390 endoplasmic reticulum stress in bile acid-induced hepatocellular injury. J Clin
391 Biochem Nutr 54:129–135.

392 Akriviadis E, Botla R, Briggs W, Han S, Reynolds T, Shakil O (2000) Pentoxifylline
393 improves short-term survival in severe acute alcoholic hepatitis: a double-blind,
394 placebo-controlled trial. Gastroenterology 119:1637–1648.

395 Almeda-Valdes P, Altamirano-Barrera A, Uribe M, Mendez-Sanchez N (2016) Metabolic
396 features of alcoholic liver disease. Rev Recent Clin Trials 11:220–226.

397 Back SH, Scheuner D, Han J, Song B, Ribick M, Wang J, Gildersleeve RD, Pennathur S,
398 Kaufman RJ (2009) Translation attenuation through eIF2alpha phosphorylation
399 prevents oxidative stress and maintains the differentiated state in beta cells. Cell
400 Metab 10:13–26.

401 Bergheim I, McClain CJ, Arteel GE (2005) Treatment of alcoholic liver disease. Dig Dis
402 23:275–284.

403 Bertola A, Mathews S, Ki SH, Wang H, Gao B (2013) Mouse model of chronic and binge
404 ethanol feeding (the NIAAA model). Nat Protoc 8:627–637.
405 Cederbaum AI (2012) ALCOHOL METABOLISM. Clin Liver Dis. 16: 667–685.
406 Cederbaum AI (2014) Methodology to assay CYP2E1 mixed function oxidase catalytic
407 activity and its induction. Redox Biol 2:1048-1054.
408 Dara L, Ji C, Kaplowitz N (2011) The contribution of endoplasmic reticulum stress to
409 liver diseases. Hepatology 53:1752–1763.
410 Fernandez A, Matias N, Fucho R, Ribas V, Von Montfort C, Nuno N, Baulies A, Martinez
411 L, Tarrats N, Mari M, et al. (2013) ASMase is required for chronic alcohol induced
412 hepatic endoplasmic reticulum stress and mitochondrial cholesterol loading. J
413 Hepatol 59:805–813.
414 Gulow K, Bienert D, Haas IG (2002) BiP is feed-back regulated by control of protein
415 translation efficiency. J Cell Sci 115:2443–2452.
416 Gurlo T, Rivera JF, Butler AE, Cory M, Hoang J, Costes S, Butler PC. (2016) CHOP
417 Contributes to, But Is Not the Only Mediator of, IAPP Induced β-Cell Apoptosis.
418 Mol Endocrinol. 30(4):446-454.
419 Gustot T, Lemmers A, Moreno C, Nagy N, Quertinmont E, Nicaise C, Franchimont D,
420 Louis H, Deviere J, Le Moine O (2006) Differential liver sensitization to toll-like

421 receptor pathways in mice with alcoholic fatty liver. Hepatology 43:989–1000.

422 Han J, Back SH, Hur J, Lin YH, Gildersleeve R, Shan J, Yuan CL, Krokowski D, Wang
423 S, Hatzoglou M, Kilberg MS, Sartor MA, Kaufman RJ (2013) ER-stress-induced
424 transcriptional regulation increases protein synthesis leading to cell death. Nat
425 Cell Biol. 15:481–490

426 Hamano M, Ezaki H, Kiso S, Furuta K, Egawa M, Kizu T, Chatani N, Kamada Y, Yoshida
427 Y, Takehara T (2014) Lipid overloading during liver regeneration causes delayed
428 hepatocyte DNA replication by increasing ER stress in mice with simple hepatic
429 steatosis. J Gastroenterol 49:305–316.

430 Hellerbrand C (2010) Pathophysiological similarities and synergisms in alcoholic and
431 non-alcoholic steatohepatitis. Dig Dis 28:783–791.

432 Hiramatsu N (2014) Translational and posttranslational regulation of XIAP by eIF2α and
433 ATF4 promotes ER stress-induced cell death during the unfolded protein response.
434 Mol Biol Cell. 25:1411-1420.

435 Hritz I, Mandrekar P, Velayudham A, Catalano D, Dolganiuc A, Kodys K, Kurt-Jones E,
436 Szabo G (2008) The critical role of toll-like receptor (TLR) 4 in alcoholic liver
437 disease is independent of the common TLR adapter MyD88. Hepatology
438 48:1224–1231.

439 Imperiale TF, McCullough AJ (1990) Do corticosteroids reduce mortality from alcoholic
440 hepatitis? A meta-analysis of the randomized trials. Ann Intern Med 113:299–307.
441 Ji C (2015) Advances and new concepts in alcohol-induced organelle stress, unfolded
442 protein responses and organ damage. Biomolecules 5:1099–1121.
443 Ji C, Kaplowitz N (2003) Betaine decreases hyperhomocysteinemia, endoplasmic
444 reticulum stress, and liver injury in alcohol-fed mice. Gastroenterology 124:1488–
445 1499.
446 Kang X, Zhong W, Liu J, Song Z, McClain CJ, Kang YJ, Zhou Z (2009) Zinc
447 supplementation reverses alcohol-induced steatosis in mice through reactivating
448 hepatocyte nuclear factor-4alpha and peroxisome proliferator-activated receptor-
449 alpha. Hepatology 50:1241–1250.
450 Kiviluoto S, Vervliet T, Ivanova H, Decuypere JP, De Smedt H, Missiaen L, Bultynck G,
451 Parys JB (2013) Regulation of inositol 1,4,5-trisphosphate receptors during
452 endoplasmic reticulum stress. Biochim Biophys Acta 1833:1612–1624.
453 Kon K, Ikejima K, Morinaga M, Kusama H, Arai K, Aoyama T, Uchiyama A, Yamashina
454 S, Watanabe S (2017) L-Carnitine prevents metabolic steatohepatitis in obese
455 diabetic KK-A(y) mice. Hepatol Res 47:E44–E54.
456 Kon K, Ikejima K, Okumura K, Arai K, Aoyama T, Watanabe S (2010) Diabetic KK-A(y)

457 mice are highly susceptible to oxidative hepatocellular damage induced by
458 acetaminophen. Am J Physiol Gastrointest Liver Physiol 299:G329–G337.
459 Kusama H, Kon K, Ikejima K, Arai K, Aoyama T, Uchiyama A, Yamashina S, Watanabe
460 S (2017) Sodium 4-phenylbutyric acid prevents murine acetaminophen
461 hepatotoxicity by minimizing endoplasmic reticulum stress. J Gastroenterol
462 52:611–622.
463 Leung TM, Nieto N (2013) CYP2E1 and oxidant stress in alcoholic and non-alcoholic
464 fatty liver disease. J Hepatol 58:395–398.
465 Mahli A, Hellerbrand C (2016) Alcohol and obesity: A dangerous association for fatty
466 liver disease. Dig Dis 34 Suppl 1:32–39.
467 Malhi H, Kaufman RJ (2011) Endoplasmic reticulum stress in liver disease. J Hepatol
468 54:795–809.
469 Malhotra JD, Miao H, Zhang K, Wolfson A, Pennathur S, Pipe SW, Kaufman RJ (2008)
470 Antioxidants reduce endoplasmic reticulum stress and improve protein secretion.
471 Proc Natl Acad Sci U S A 105:18525–18530.
472 Mathurin P, O'Grady J, Carithers RL, Phillips M, Louvet A, Mendenhall CL, Ramond
473 MJ, Naveau S, Maddrey WC, Morgan TR (2011) Corticosteroids improve short-
474 term survival in patients with severe alcoholic hepatitis: meta-analysis of

475 individual patient data. Gut 60:255–260.

476 Morinaga M, Kon K, Saito H, Arai K, Kusama H, Uchiyama A, Yamashina S, Ikejima K,
477 Watanabe S (2015) Sodium 4-phenylbutyrate prevents murine dietary
478 steatohepatitis caused by trans-fatty acid plus fructose. J Clin Biochem Nutr
479 57:183–191.

480 Naveau S, Giraud V, Borotto E, Aubert A, Capron F, Chaput JC (1997) Excess weight
481 risk factor for alcoholic liver disease. Hepatology 25:108–111.

482 Okumura K, Ikejima K, Kon K, Abe W, Yamashina S, Enomoto N, Takei Y, Sato N (2006)
483 Exacerbation of dietary steatohepatitis and fibrosis in obese, diabetic KK-A(y)
484 mice. Hepatol Res 36:217–228.

485 Petrasek J, Bala S, Csak T, Lippai D, Kodys K, Menashy V, Barrieau M, Min SY, Kurt-
486 Jones EA, Szabo G (2012) IL-1 receptor antagonist ameliorates inflammasome-
487 dependent alcoholic steatohepatitis in mice. J Clin Invest 122:3476–3489.

488 Raff EJ, Kakati D, Bloomer JR, Shoreibah M, Rasheed K, Singal AK (2015) Diabetes
489 mellitus predicts occurrence of cirrhosis and hepatocellular cancer in alcoholic
490 liver and non-alcoholic fatty liver diseases. J Clin Transl Hepatol 3:9–16.

491 Rehm J, Samokhvalov AV, Shield KD (2013) Global burden of alcoholic liver diseases. J
492 Hepatol 59:160–168.

493 Rolo AP, Teodoro JS, Palmeira CM (2012) Role of oxidative stress in the pathogenesis of
494 nonalcoholic steatohepatitis. Free Radic Biol Med 52:59–69.
495 Roy D, Kumar V, James J, Shihabudeen MS, Kulshrestha S, Goel V, Thirumurugan K
496 (2015) Evidence that chemical chaperone 4-phenylbutyric acid binds to human
497 serum albumin at fatty acid binding sites. PLoS One 10:e0133012.
498 Roychowdhury S, McMullen MR, Pritchard MT, Hise AG, van Rooijen N, Medof ME,
499 Stavitsky AB, Nagy LE (2009) An early complement-dependent and TLR-4-
500 independent phase in the pathogenesis of ethanol-induced liver injury in mice.
501 Hepatology 49:1326–1334.
502 Sasaki M, Yoshimura-Miyakoshi M, Sato Y, Nakanuma Y (2015) A possible involvement
503 of endoplasmic reticulum stress in biliary epithelial autophagy and senescence in
504 primary biliary cirrhosis. J Gastroenterol 50:984–995.
505 Shen Z, Liang X, Rogers CQ, Rideout D, You M (2010) Involvement of adiponectin-
506 SIRT1-AMPK signaling in the protective action of rosiglitazone against alcoholic
507 fatty liver in mice. Am J Physiol Gastrointest Liver Physiol 298:G364–374.
508 Southwood CM, Fykkolodziej B, Maheras KJ, Garshott DM, Estill M, Fribley AM, Gow
509 A (2016) Overexpression of CHOP in Myelinating Cells Does Not Confer a
510 Significant Phenotype under Normal or Metabolic Stress Conditions. J Neurosci.

511 36:6803-6819.

512 Szuster-Ciesielska A, Mizerska-Dudka M, Daniluk J, Kandefer-Szerszen M (2013)
513 Butein inhibits ethanol-induced activation of liver stellate cells through TGF-beta,
514 NFkappaB, p38, and JNK signaling pathways and inhibition of oxidative stress. J
515 Gastroenterol 48:222–237.

516 Takashima S, Ikejima K, Arai K, Yokokawa J, Kon K, Yamashina S, Watanabe S (2016)
517 Glycine prevents metabolic steatohepatitis in diabetic KK-Ay mice through
518 modulation of hepatic innate immunity. Am J Physiol Gastrointest Liver Physiol
519 311:G1105–1113.

520 Tan TC, Crawford DH, Jaskowski LA, Subramaniam VN, Clouston AD, Crane DI, Bridle
521 KR, Anderson GJ, Fletcher LM (2013) Excess iron modulates endoplasmic
522 reticulum stress-associated pathways in a mouse model of alcohol and high-fat
523 diet-induced liver injury. Lab Invest 93:1295–1312.

524 Tilg H, Moschen AR (2010) Evolution of inflammation in nonalcoholic fatty liver
525 disease: the multiple parallel hits hypothesis. Hepatology 52:1836–1846.

526 Tsukamoto H (2007) Conceptual importance of identifying alcoholic liver disease as a
527 lifestyle disease. J Gastroenterol 42:603–609.

528 Watanabe S, Hashimoto E, Ikejima K, Uto H, Ono M, Sumida Y, Seike M, Takei Y,

529 Takehara T, Tokushige K, et al. (2015a) Evidence-based clinical practice
530 guidelines for nonalcoholic fatty liver disease/nonalcoholic steatohepatitis. J
531 Gastroenterol 50:364–377.
532 Watanabe S, Hashimoto E, Ikejima K, Uto H, Ono M, Sumida Y, Seike M, Takei Y,
533 Takehara T, Tokushige K, et al. (2015b) Evidence-based clinical practice
534 guidelines for nonalcoholic fatty liver disease/nonalcoholic steatohepatitis.
535 Hepatol Res 45:363–377.
536 Wu D, Wang X, Zhou R, Yang L, Cederbaum AI (2012) Alcohol steatosis and
537 cytotoxicity: the role of cytochrome P4502E1 and autophagy. Free Radic Biol
538 Med 53:1346–1357.
539 Yamagata H, Ikejima K, Takeda K, Aoyama T, Kon K, Okumura K, Watanabe S (2013)
540 Altered expression and function of hepatic natural killer T cells in obese and
541 diabetic KK-A(y) mice. Hepatol Res 43:276–288.
542 Yamaguchi H, Wang HG (2004) CHOP is involved in endoplasmic reticulum stress-
543 induced apoptosis by enhancing DR5 expression in human carcinoma cells. J Biol
544 Chem 279:45495–45502.
545 Yamashina S, Takei Y, Ikejima K, Enomoto N, Kitamura T, Sato N (2005) Ethanol-
546 induced sensitization to endotoxin in Kupffer cells is dependent upon oxidative

547 stress. Alcohol Clin Exp Res 29:246s–250s.

548 Yang L, Wu D, Wang X, Cederbaum AI (2012) Cytochrome P4502E1, oxidative stress,

549 JNK, and autophagy in acute alcohol-induced fatty liver. Free Radic Biol Med

550 53:1170–1180.

551 Yu CH, Xu CF, Ye H, Li L, Li YM (2010) Early mortality of alcoholic hepatitis: a review

552 of data from placebo-controlled clinical trials. World J Gastroenterol 16:2435–

553 2439.

554 Zhou H, Liu R (2014) ER stress and hepatic lipid metabolism. Front Genet. 5: 112.

555

556 **Figure 1. Effect of 4-PBA on steatohepatitis in chronic-plus-binge EtOH-fed KK-A^{y}**

557 **mice.** Mice were fed EtOH or pair-fed a control diet for 10 days. Some mice were treated

558 with PBA (120 mg/kg body weight by intraperitoneal injection) and then given an EtOH

559 gavage (4 g/kg body weight) on day 11, and sacrificed 9 h later. (A) Body weight change

560 during the experimental period. (B-C) Average blood sugar (B) and serum triglyceride

561 (C) levels determined colorimetrically. (D–F) Representative photomicrographs of H-E

562 staining of liver tissues from control (D), EtOH (E), or EtOH + PBA (F) mice

563 (magnification: 100×, scale bar = 100 μm). Yellow arrowheads indicate infiltrated

564 neutrophils. (G) Higher-magnification image of (E) (400×, scale bar = 100 μm). (H)

565 Average liver triglyceride content per liver weight. (I–J) Average serum AST and ALT

566 levels determined colorimetrically. *$P < 0.05$ vs. control; $^{\#}P < 0.05$ vs. EtOH (ANOVA

567 and Student–Neuman–Keuls post-hoc test, n = 5).

568

569 **Figure 2. Effect of 4-PBA on hepatocyte apoptosis and inflammation caused by**

570 **EtOH feeding.** Experimental design is the same as in Fig.1. (A–C) Representative

571 photomicrographs of liver tissue from control (A), EtOH (B), or EtOH + PBA (C) mice

572 are shown (ccCK18 immunolabeling; magnification: 100×, scale bar = 100 μm). Yellow

573 arrow heads indicate ccCK positive hepatocytes. (D) The number of ccCK18-positive

574 cells was counted and average percentages of ccCK18-positive hepatocytes/total
575 hepatocytes from five different animals are plotted. More than five fields per animal were
576 evaluated. (E, F) Hepatic mRNA expression of *TNFα* (E) and *IL6* (F) was evaluated by
577 qPCR. *P < 0.05 vs. control; #P < 0.05 vs. EtOH (ANOVA and Student–Neuman–Keuls
578 post-hoc test, n = 5)
579
580 **Figure 3. Effect of 4-PBA on ER stress in the liver of KK-A^y mice subjected to**
581 **chronic-plus-binge EtOH feeding.** (A–E) Experimental design is the same as in Fig.1.
582 Hepatic mRNA expression of *BiP* (A), *uXBP-1* (B), *sXBP-1* (C), *IP3R1* (D), and *CHOP*
583 (E) was evaluated by qPCR. (F) The expression of CHOP in protein levels was measured
584 by western blotting. A representative band images of western blot are shown in the upper
585 row, and the averages of densitometry values standardized relative to GAPDH for each
586 condition were expressed relative to control are plotted. *P < 0.05 vs. control; #P < 0.05
587 vs. EtOH (ANOVA and Student–Neuman–Keuls post-hoc test, n = 5).
588
589 **Figure 4. Effect of 4-PBA on oxidative stress in the liver of KK-A^y mice subjected to**
590 **chronic-plus-binge EtOH feeding.** Experimental design is the same as in Fig.1. (A–C)
591 Representative photomicrographs of liver tissue from control (A), EtOH (B), or EtOH +

592 PBA (C) mice are shown (4-HNE immunolabeling; magnification: 100×, scale bar = 100
593 μm). (D) The number of 4-HNE-positive cells was counted and average percentages of
594 4-HNE-stained hepatocytes from five different animals are plotted. More than five fields
595 of per animal were evaluated. (E) Hepatic mRNA expression of *HO-1* was evaluated by
596 qPCR. *P < 0.05 vs. control; #P < 0.05 vs. EtOH (ANOVA and Student–Neuman–Keuls
597 post-hoc test, n = 5).
598
599 **Figure 5. Effect of 4-PBA on liver injury in KK-A^y mice subjected to chronic EtOH**
600 **feeding.** Mice were fed EtOH or pair-fed a control diet for 10 days, then sacrificed on day
601 11 without an EtOH binge. Some mice were treated with PBA (120 mg/kg body weight
602 by intraperitoneal injection). (A–F) Hepatic mRNA expression of *BiP* (A), *uXBP-1* (B),
603 *sXBP-1* (C), *IP3R1* (D), and *CHOP* (E) was evaluated by qPCR. (F) The expression of
604 CHOP in protein levels was measured by western blotting. A representative band images
605 of western blot are shown in the upper row, and the averages of densitometry values
606 standardized relative to GAPDH for each condition were expressed relative to control are
607 plotted. (G) Hepatic mRNA expression of *HO-1* was evaluated by qPCR. (H and I) Serum
608 AST and ALT levels were determined colorimetrically. (H) *P < 0.05 vs. control; #P <
609 0.05 vs. EtOH (ANOVA and Student–Neuman–Keuls post-hoc test, n = 5).

610

611 **Figure 6. Effect of 4-PBA on activity of CYP2E1 in KK-A^y mice subjected to chronic**

612 **EtOH feeding.** Experimental design is the same as in Fig.5. (A) Hepatic mRNA

613 expression of CYP2E1 was evaluated by qPCR. (B) Hepatic CYP2E1 activity was

614 measured by the rate of oxidation of p-nitrophenol to p-nitrocatechol. *$P < 0.05$ vs.

615 control (ANOVA and Student–Neuman–Keuls post-hoc test, $n = 5$).

Gene name	GenBank accession number	forward	reverse
CHOP	NM_007837.4	AGTGCATCTTCATACACCACCACA,	CAGATCCTCATACCAGGCTTCCA
sXBP1	NM_001271730.1	TGAGAACCAGGAGTTAAGAACACGC	CCTGCACCTGCTGCGGAC
uXBP1	NM_013842.3	TGTGGTTGAGAACCAGGAGTTAAGA	CTGCTGCAGAGGTGCACATAG
CYP2E1	NM_021282	CATGGCTACAAGGCTGTCAA	CCAGGGAGTACTCAGCAGGT
HO-1	NM_010442.2	CTGGAGATGACACCTGAGGTCAA	CTGACGAAGTGACGCCATCTG
TNFα	NM_013693.2	GTTCTATGGCCCAGACCCTCAC	GGCACCACTAGTTGGTTGTCTTTG
IL6	NM_031168.1	CCACTTCACAAGTCGGAGGCTTA	GCAAGTGCATCATCGTTGTTCATAC
IP3R1	NM_010585.5	GGTCAGCAGCGATTCTGGAGG	TGGGTTGACATTCATGTGAGG
BiP	NM_001163434.1	GAACACTGTGGTACCCACCAAGAA	TCCAGTCAGATCAAATGTACCCAGA
GAPDH	NM_008084.2	TGTGTCCGTCGTGGATCTGA	TTGCTGTTGAAGTCGCAGGAG).

628 **Table 1. List of forward and reverse primers used for gene expression analysis**
629 **through RT-PCR**

630 CHOP: C/EBP homologous protein, sXBP1: spliced X-box-binding protein-1, uXBP1:
631 unspliced X-box-binding protein-1, CYP2E1: cytochrome P450 2E1, HO-1: heme
632 oxygenase-1, TNFα: tumor necrosis factor α, IL6: interleukin 6, IP3R1: inositol
633 trisphosphate receptor, BiP, GAPDH: glyceraldehyde 3-phosphate dehydrogenase.

634

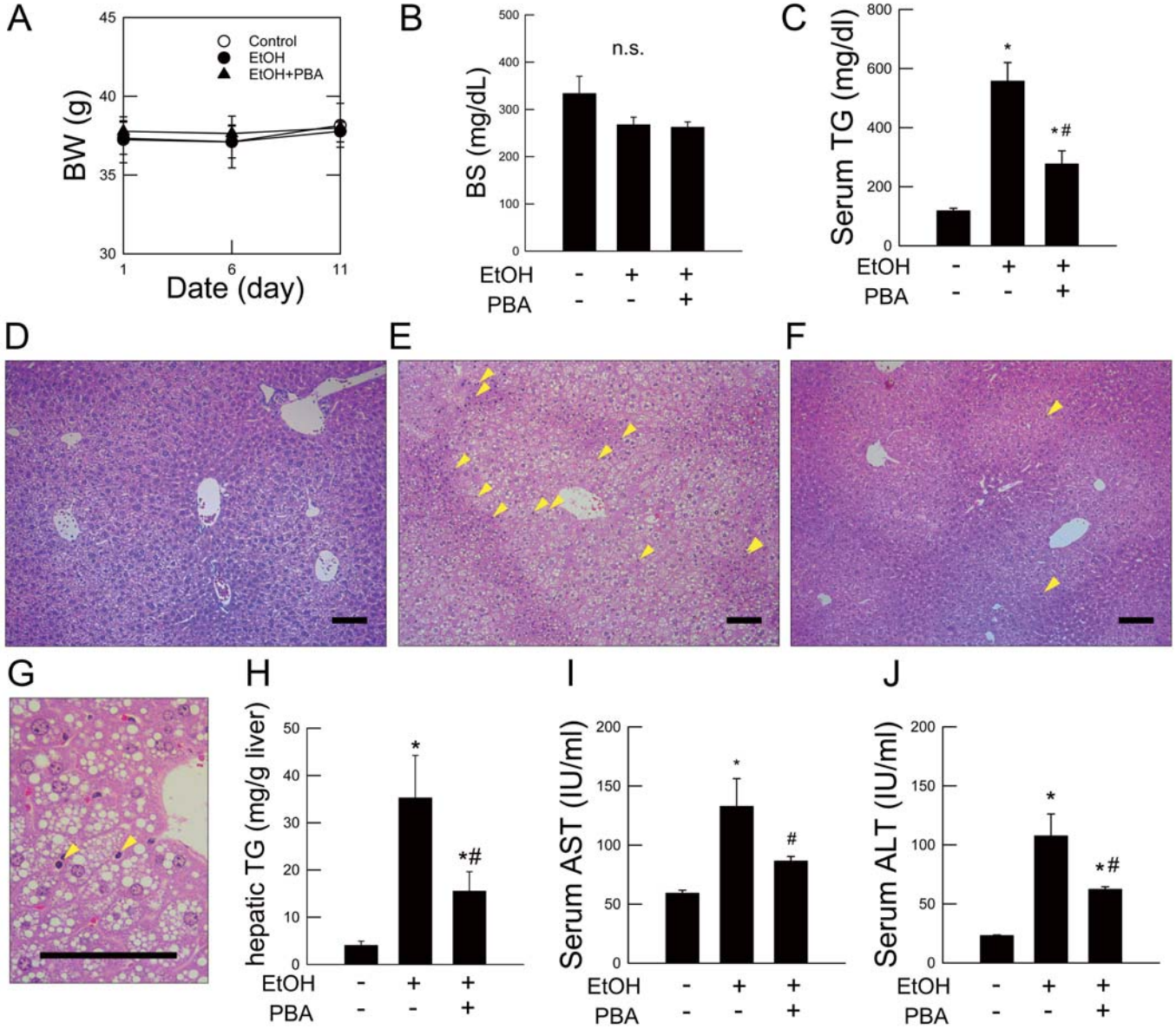
A
Control
EtOH
EtOH+PBA
BW (g)
Date (day)
B
n.s.
BS (mg/dL)
EtOH
PBA
C
Serum TG (mg/dl)
EtOH
PBA
D
E
F
G
H
hepatic TG (mg/g liver)
EtOH
PBA
I
Serum AST (IU/ml)
EtOH
PBA
J
Serum ALT (IU/ml)
EtOH
PBA

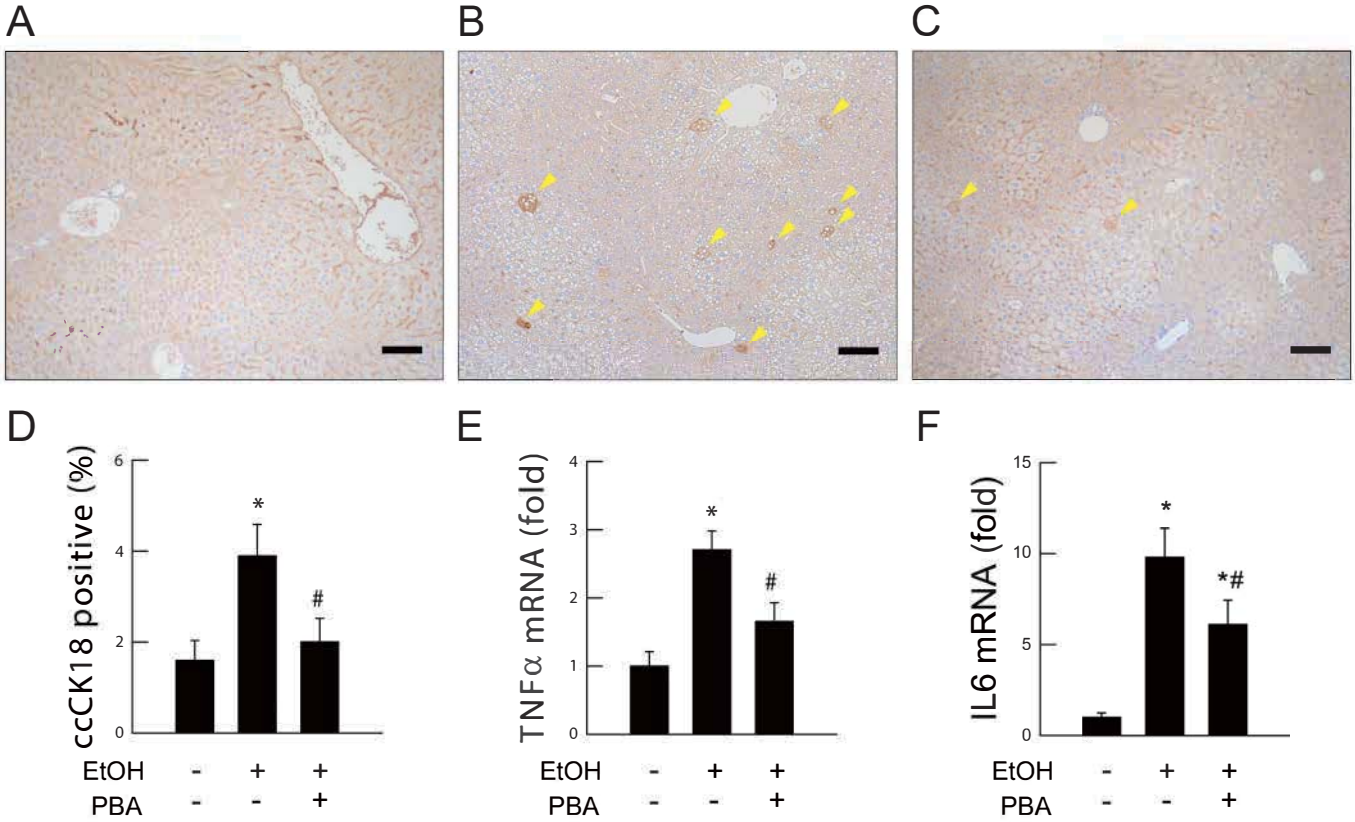
A
B
C
D
ccCK18 positive (%)
0
2
4
6
*
#
EtOH - + +
PBA - - +
E
TNFα mRNA (fold)
0
1
2
3
4
*
#
EtOH - + +
PBA - - +
F
IL6 mRNA (fold)
0
5
10
15
*
*#
EtOH - + +
PBA - - +

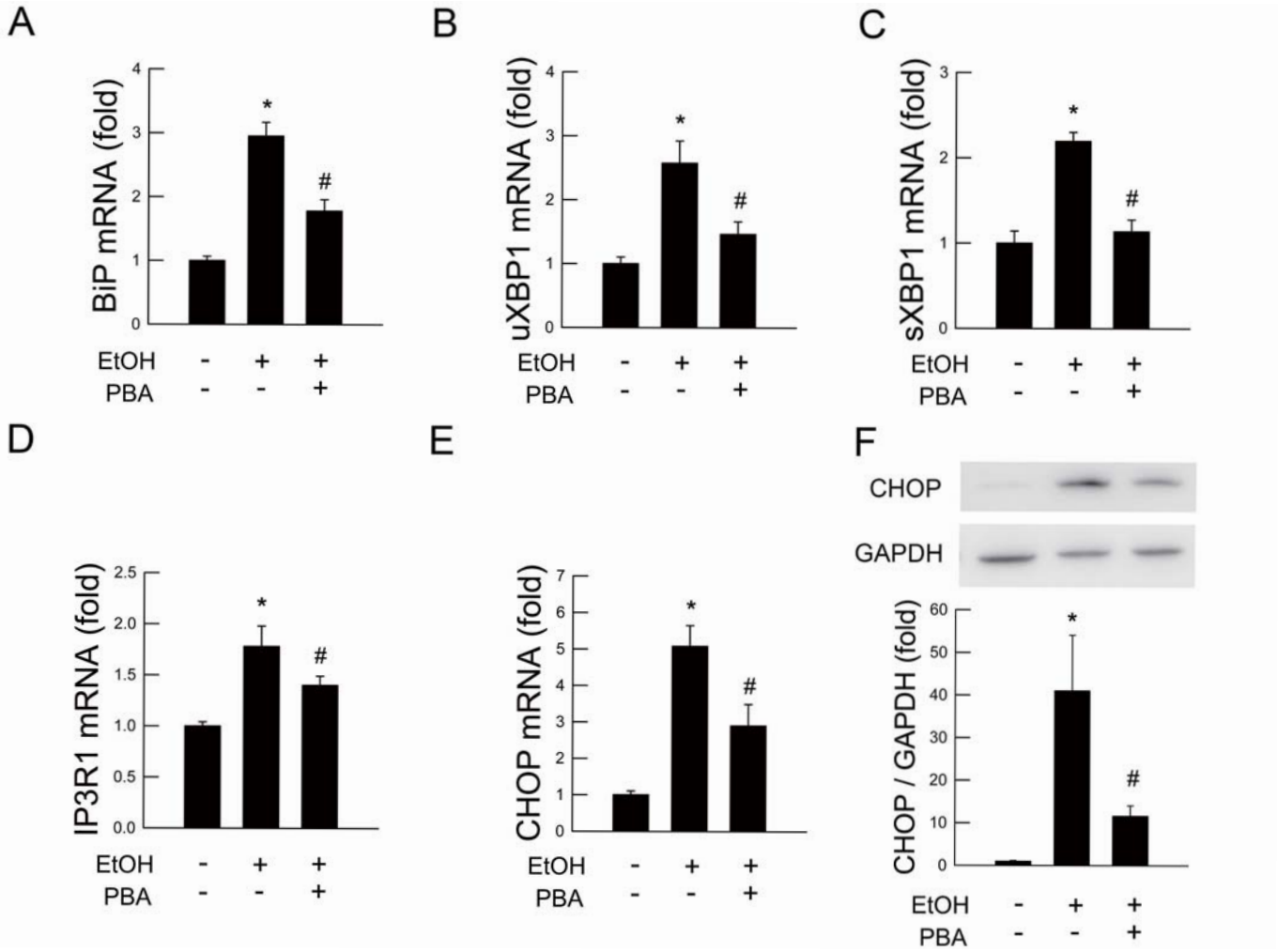
A
BiP mRNA (fold)
0
1
2
3
4
*
#
EtOH - + +
PBA - - +
B
uXBP1 mRNA (fold)
0
1
2
3
4
*
#
EtOH - + +
PBA - - +
C
sXBP1 mRNA (fold)
0
1
2
3
*
#
EtOH - + +
PBA - - +
D
IP3R1 mRNA (fold)
0.0
0.5
1.0
1.5
2.0
2.5
*
#
EtOH - + +
PBA - - +
E
CHOP mRNA (fold)
0
1
2
3
4
5
6
7
*
#
EtOH - + +
PBA - - +
F
CHOP
GAPDH
CHOP / GAPDH (fold)
0
10
20
30
40
50
60
*
#
EtOH - + +
PBA - - +

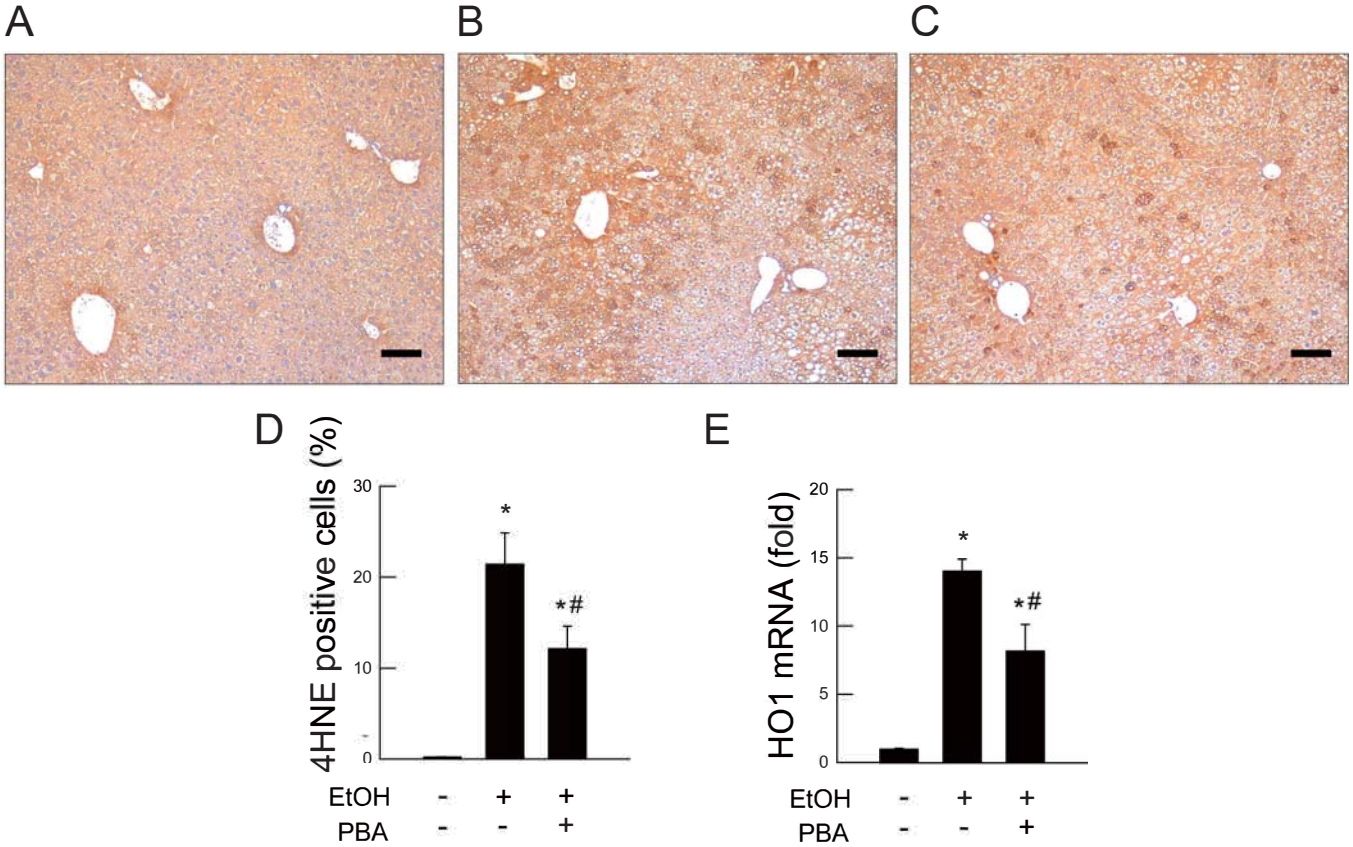
A
B
C
D
4HNE positive cells (%)
30
20
10
0
*
*#
EtOH - + +
PBA - - +
E
HO1 mRNA (fold)
20
15
10
5
0
*
*#
EtOH - + +
PBA - - +

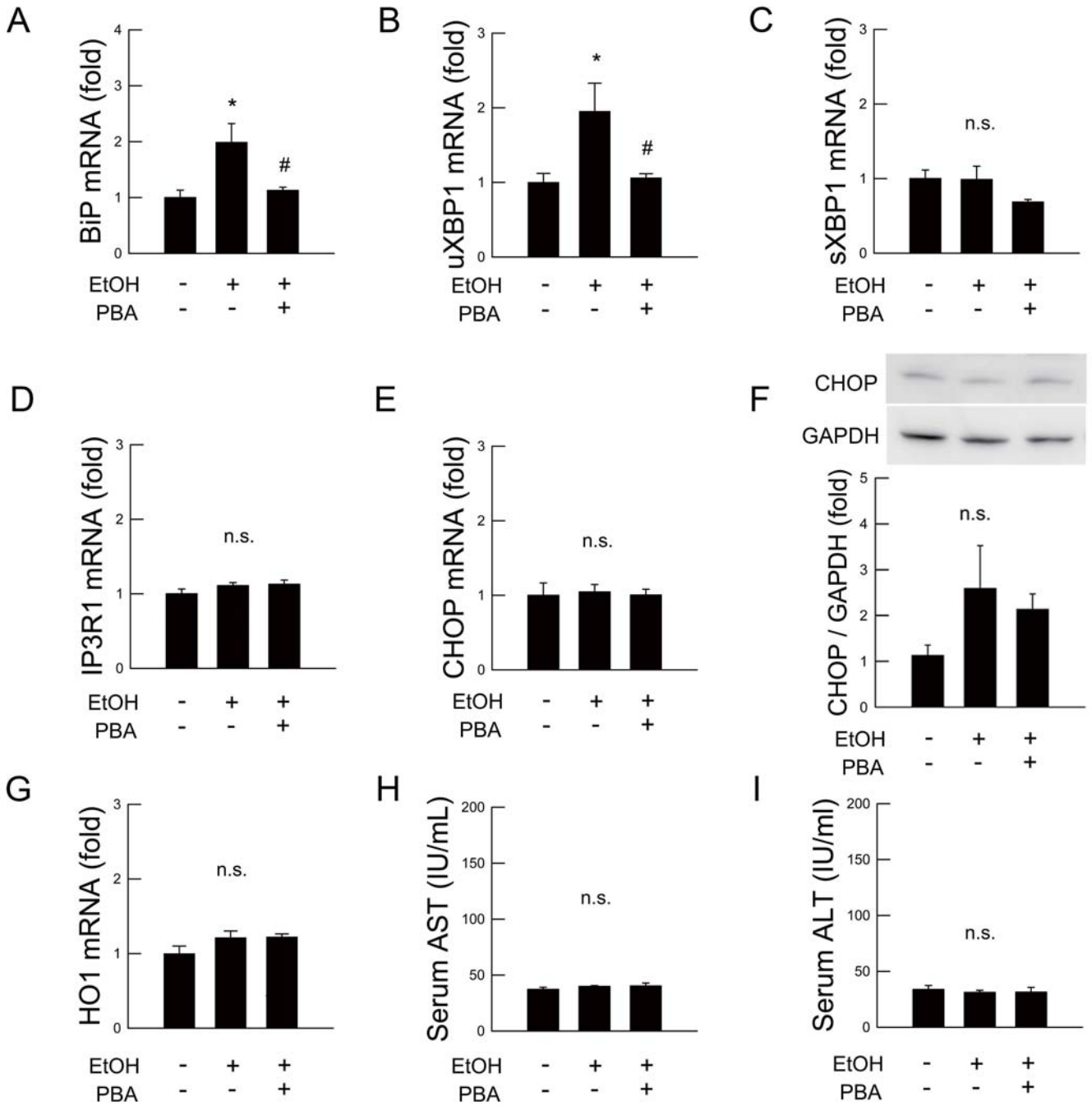
A
BiP mRNA (fold)
0
1
2
3
4
*
#
EtOH - + +
PBA - - +
B
uXBP1 mRNA (fold)
0
1
2
3
*
#
EtOH - + +
PBA - - +
C
sXBP1 mRNA (fold)
0
1
2
3
n.s.
EtOH - + +
PBA - - +
D
IP3R1 mRNA (fold)
0
1
2
3
n.s.
EtOH - + +
PBA - - +
E
CHOP mRNA (fold)
0
1
2
3
n.s.
EtOH - + +
PBA - - +
F
CHOP
GAPDH
CHOP / GAPDH (fold)
0
1
2
3
4
5
n.s.
EtOH - + +
PBA - - +
G
HO1 mRNA (fold)
0
1
2
3
n.s.
EtOH - + +
PBA - - +
H
Serum AST (IU/mL)
0
50
100
150
200
n.s.
EtOH - + +
PBA - - +
I
Serum ALT (IU/ml)
0
50
100
150
200
n.s.
EtOH - + +
PBA - - +

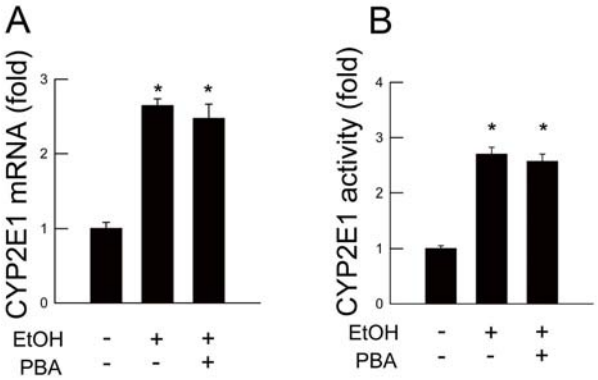
A
CYP2E1 mRNA (fold)
0
1
2
3
*
*
EtOH - + +
PBA - - +
B
CYP2E1 activity (fold)
0
1
2
3
4
*
*
EtOH - + +
PBA - - +

Supplementary figure 1. Pathological change in C57Bl/6J mice subjected to chronic-plus-binge EtOH feeding. C57Bl6 mice were fed EtOH or pair-fed a control diet for 10 days, Mice were given an EtOH gavage (5 g/kg body weight) on day 11, then sacrificed 9 h later. Representative photomicrograph of H-E staining of liver tissue is shown (magnification: 100×, scale bar = 100 μm).